

# Heat capacity of aqueous mixtures of monoethanolamine with 2-piperidineethanol

Tzn-Wei Shih, Yan-Jen Chen, Meng-Hui Li\*

Department of Chemical Engineering, Chung Yuan Christian University, Chung Li 32023, Taiwan, ROC

Received 15 August 2001; received in revised form 28 December 2001; accepted 1 January 2002

## Abstract

The binary system studied was monoethanolamine (MEA) + 2-piperidineethanol (2-PE). Heat capacities of aqueous mixtures of MEA with 2-PE were measured from 30 to 80 °C with a differential scanning calorimeter (DSC). For mole fractions of water ranging from 0.2 to 0.8, 16 concentrations of the MEA + 2-PE + water systems were studied. An excess molar heat capacity expression, using the Redlich–Kister equation for the composition dependence, is used to represent the measured  $C_p$  of alkanolamine aqueous solutions. The results of heat capacity calculation (overall average absolute percentage deviation) for a total of 176 data points for MEA + 2-PE + water system are 0.2 and 7.4% for molar heat capacity and excess molar heat capacity, respectively. The heat capacity values of aqueous mixtures of MEA with 2-PE presented in this study are, in general, of sufficient accuracy for most engineering-design calculations when using MEA + 2-PE + water as absorbent for acid gas removal process. © 2002 Elsevier Science B.V. All rights reserved.

**Keywords:** Heat capacity; Alkanolamines; Monoethanolamine; 2-Piperidineethanol

## 1. Introduction

Acid gas impurities ( $\text{CO}_2$  and  $\text{H}_2\text{S}$ ) are commonly removed from natural gas, synthetic and refinery gas streams by absorption into aqueous alkanolamine solutions. Alkanolamines such as monoethanolamine (MEA), diglycolamine (DGA), diethanolamine (DEA), diisopropanolamine (DIPA), triethanolamine (TEA) and *N*-methyldiethanolamine (MDEA), 2-amino-2-methyl-1-propanol (AMP) and 2-piperidineethanol (2-PE) are indicated to be used as an absorbent for acid gas removal processes [1].

Heat-capacity data for alkanolamine solutions are required for the design of the heat-exchanger equip-

ment used in gas treating processes. The heat capacities of pure alkanolamines have been reported in the literature [2–6]. Some heat capacities of aqueous alkanolamine solutions are also available in the literature: MEA +  $\text{H}_2\text{O}$  [7–9]; DGA +  $\text{H}_2\text{O}$  [9,10], DEA +  $\text{H}_2\text{O}$  [7–9]; DIPA +  $\text{H}_2\text{O}$  [9]; TEA +  $\text{H}_2\text{O}$  [9]; MDEA +  $\text{H}_2\text{O}$  [8,9,11]; AMP +  $\text{H}_2\text{O}$  [9] and 2-PE +  $\text{H}_2\text{O}$  [9]. At 25 °C, heat capacities of  $\text{CO}_2$ -loaded, aqueous solutions of MEA, DEA, MDEA, aqueous MDEA + MEA and MDEA + DEA were also studied [8]. For the blend-alkanolamine aqueous solutions, heat capacities of MEA + MDEA +  $\text{H}_2\text{O}$  [8,12], MEA + AMP +  $\text{H}_2\text{O}$  [13], DEA + MDEA +  $\text{H}_2\text{O}$  [8] and DEA + AMP +  $\text{H}_2\text{O}$  [14] have also been studied for temperature over 30–80 °C. For the MEA + 2-PE +  $\text{H}_2\text{O}$  system, the heat capacity, however, has not yet been reported in the literature. Thus, it is the purpose of this study to determine

\* Corresponding author. Tel.: +886-3-456-3171/4110;  
fax: +886-3-456-3171/4199.  
E-mail address: mhli@cycu.edu.tw (M.-H. Li).

experimentally the heat capacities of MEA + 2-PE + H<sub>2</sub>O as a function of mole percent of water and different temperatures by using a differential scanning calorimeter (DSC). Using the Redlich–Kister equation for the concentration dependence, an excess molar heat capacity expression will be applied to represent the measured  $C_p$  data.

## 2. Experimental

MEA is Riedel-de Haën reagent grade with the purity minimum 99% (water maximum 0.5%) and 2-PE is Acros Organics reagent grade with the purity +95%. The water is liquid chromatography grade from Alps Chemical Co.

The differential scanning calorimeter used for this study consists of a DSC-2010 and a thermal analysis controller from TA Instruments. The DSC operating range is from the room temperature to 725 °C. Both the temperatures and the heat flow associated with transitions in materials can be easily and rapidly measured with the system. The DSC features a temperature of  $\pm 0.1$  °C repeatability. Calorimetric sensitivity is 1  $\mu$ W (rms). The purge gas is nitrogen with a flow rate of 40 ml min<sup>-1</sup>. By using the sample encapsulating press, the liquid sample was prepared within a hermetic sample pan. The internal volume of the hermetic pan is approximately 10 mm<sup>3</sup>. Sample weight is in the range of 15–20 mg. The accuracy of the  $C_p$  measurements is estimated to be  $\pm 2\%$  based on the measurement of  $C_p$  of liquid water [6]. The apparatus and the experimental procedure are the same as those described by Chiu et al. [6].

## 3. Results and discussion

The values of  $C_p$  of MEA (1) + 2-PE (2) have been measured for temperatures from 30 to 80 °C and are presented in Table 1.

An excess molar heat capacity  $C_p^E$  for a mixture is defined [15] as

$$C_p^E = C_p - \sum_i x_i C_{p,i} \quad (1)$$

where  $C_{p,i}$  (J mol<sup>-1</sup> K<sup>-1</sup>) is the molar heat capacity of the pure component  $i$ . In this study, the molar heat

Table 1  
Heat Capacities (J mol<sup>-1</sup> K<sup>-1</sup>) of MEA (1) + 2-PE (2)

$t$ (°C)	$x_1 = 0.2$		$x_1 = 0.4$		$x_1 = 0.6$		$x_1 = 0.8$	
	$C_p$	$C_p^E$	$C_p$	$C_p^E$	$C_p$	$C_p^E$	$C_p$	$C_p^E$
30	272	4.2	249	6.4	223	5.6	197	4.8
35	275	3.6	251	5.2	226	5.8	198	3.4
40	278	4.0	254	6.0	228	6.0	200	4.0
45	281	3.4	256	4.8	230	5.2	202	3.6
50	284	3.0	259	5.0	232	5.0	204	4.0
55	287	3.2	261	4.4	234	4.6	205	2.8
60	290	2.8	264	4.6	236	4.4	207	3.2
65	292	1.2	266	3.4	238	3.6	209	2.8
70	295	1.6	269	4.2	240	3.8	211	3.4
75	298	1.2	271	3.4	242	3.6	212	2.8
80	301	0.6	274	3.2	245	3.8	214	2.4

capacity of water is from Osborne et al. [16] and the molar heat capacity of MEA and 2-PE are Chiu et al. [6]. The derived values of  $C_p^E$  from Eq. (1) are also presented in Table 1. The plot of  $C_p^E$  versus  $x_1$  for MEA (1) + 2-PE (2) is shown in Fig. 1. In Fig. 1, the points represent the derived excess molar heat capacity calculated from Eq. (1). The values of  $C_p^E$  for MEA (1) + 2-PE (2) exhibit all positive values over the entire concentration range, as shown in Fig. 1. The temperature dependence of  $C_p^E$  for low concentration of MEA, i.e.  $x_1 = 0.2$ , is stronger than that for high concentration of MEA, i.e.  $x_1 = 0.8$ , as shown in Fig. 1.

To represent the compositional dependence of the excess molar heat capacity for a binary mixture, a Redlich–Kister equation was applied as follows:

$$C_{p,12}^E / (\text{J mol}^{-1} \text{K}^{-1}) = x_1 x_2 \sum_{i=1}^n A_i (x_1 - x_2)^{i-1} \quad (2)$$

The temperature dependence of  $A_i$  is assumed to follow the equation

$$A_i = a_{i,0} + a_{i,1}(T/\text{K})$$

where  $T$  is in Kelvin.

The parameters  $a_{i,0}$  and  $a_{i,1}$  are determined from the values of  $C_{p,12}^E$  for MEA (1) + 2-PE (2) and are presented in Table 2. For a total of 44 data points, the overall AAD% for the calculation of heat capacity for MEA (1) + 2-PE (2) are 9.7 and 0.1% for  $C_p^E$  and  $C_p$ , respectively. In Fig. 1, a comparison between the calculated values, from Eq. (2) and the derived values,

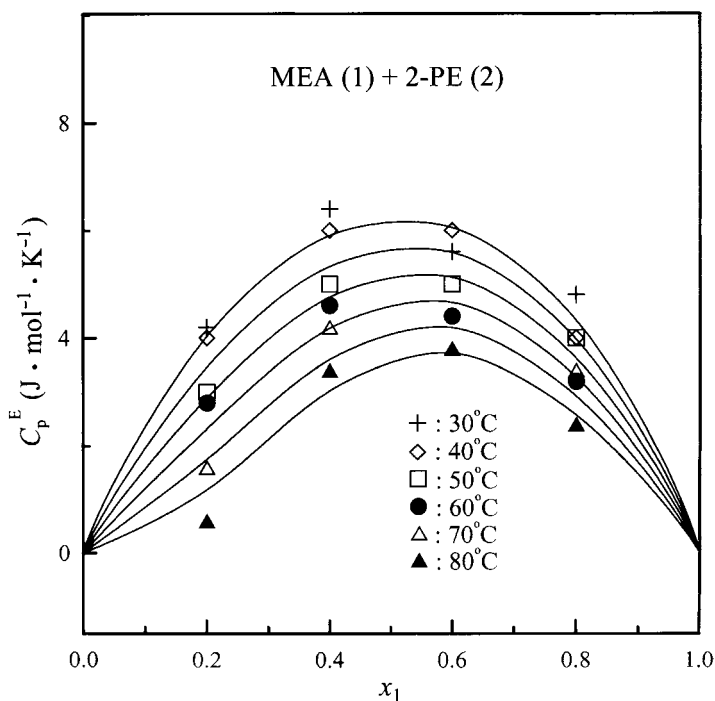


Fig. 1. Excess molar heat capacity of MEA (1) + 2-PE (2): symbols, derived values; lines, calculated using Eq. (2).

from Eq. (1), of  $C_p^E$  for MEA (1) + 2-PE (2) is shown. For the calculation of  $C_p^E$  for the ternary system, the parameters for all three binaries are normally required. The parameters  $a_{i,0}$  and  $a_{i,1}$  for  $C_p^E$  of binaries

MEA + H<sub>2</sub>O [12] and 2-PE + H<sub>2</sub>O [9] are also listed in Table 2 for reference.

In Fig. 2, a comparison of  $C_p^E$  for binary mixtures of MEA with MDEA, AMP and 2-PE at 50 °C are shown.

Table 2  
Parameters of excess molar heat capacity for binary and ternary systems

Binary system	Parameters			No. of data points	AAD (%) <sup>c</sup>	
	$i$	$a_{i,0}$	$a_{i,1}$		$C_p^E$	$C_p$
MEA (1) + H <sub>2</sub> O (2) <sup>a</sup>	1	-146.65	0.4898			
	2	22.60	-0.0790			
	3	10.88	-0.0532			
2-PE (1) + H <sub>2</sub> O (2) <sup>b</sup>	1	-111.96	0.4285			
	2	46.933	-0.1834			
MEA (1) + 2-PE (2)	1	87.975	-0.209	44	9.7	0.1
	2	-32.977	0.1138			
	3	70.51	-0.2202			
Ternary system		$b_{1,0}$	$b_{1,1}$			
MEA (1) + 2-PE (2) + H <sub>2</sub> O (3)		-59.16	0.1626	176	7.4	0.2

<sup>a</sup> Values of Chen et al. [12].

<sup>b</sup> Values of Chiu and Li [9].

<sup>c</sup> AAD (%): average absolute percentage deviation.

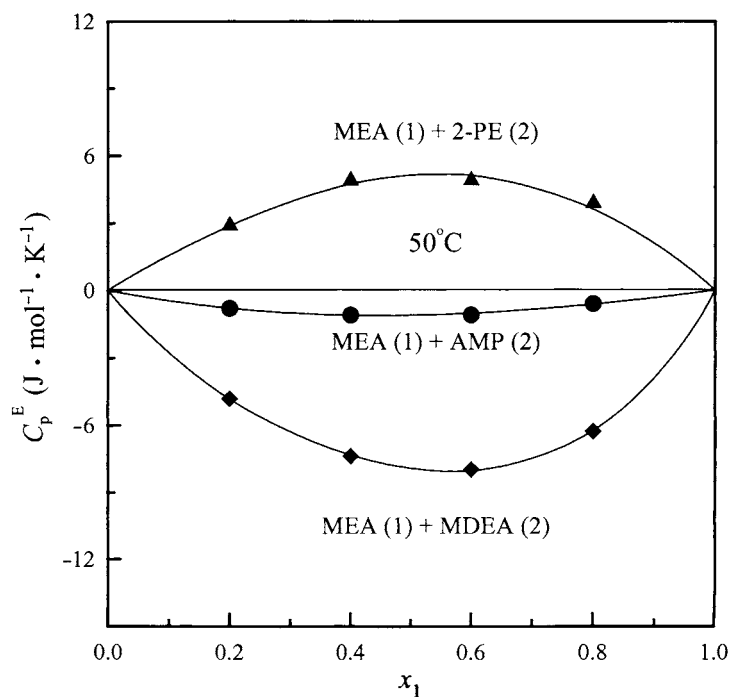


Fig. 2. Excess molar heat capacity of three binaries at 50 °C: symbols, derived values, MEA + MDEA [12], MEA + AMP [13]; lines, calculated using Eq. (2).

The values of  $C_p^E$  for MEA (1) + MDEA (2) are from Chen et al. [12] and for MEA (1) + AMP (2) from Chen and Li [13]. As shown in Fig. 2, the values of  $C_p^E$  for MEA (1) + MDEA (2) show negative values while those for MEA (1) + 2-PE (2) positives values. It indicates that the solution of MEA (primary amine) + MDEA (tertiary amine) exhibits a higher

degree of non-ideality than that for the system MEA (primary amine) + AMP (sterically hindered primary amine). Also, the molecular interactions between MEA and MDEA are quite different from those between MEA and 2-PE.

The  $C_p$  of MEA (1) + 2-PE (2) + H<sub>2</sub>O (3) were also measured for temperatures over 30–80 °C and for

Table 3

Heat capacities ( $J \text{ mol}^{-1} \text{ K}^{-1}$ ) of MEA (1) + 2-PE (2) + H<sub>2</sub>O (3) for  $x_3 = 0.8$

$t$ (°C)	$x_1/x_2 = 0.04/0.16$		$x_1/x_2 = 0.08/0.12$		$x_1/x_2 = 0.12/0.08$		$x_1/x_2 = 0.16/0.04$	
	$C_p$	$C_p^E$	$C_p$	$C_p^E$	$C_p$	$C_p^E$	$C_p$	$C_p^E$
30	117	3.2	111	2.3	105	1.3	100	1.4
35	118	3.5	112	2.6	106	1.8	101	1.9
40	119	4.0	113	3.2	107	2.4	101	1.6
45	120	4.3	114	3.5	108	2.8	102	2.1
50	121	4.6	115	4.0	109	3.4	103	2.8
55	123	6.0	116	4.4	110	3.9	104	3.3
60	124	6.3	117	4.8	111	4.4	105	4.0
65	125	6.5	118	5.2	112	4.8	105	3.4
70	126	7.0	119	5.7	113	5.4	106	4.1
75	127	7.2	120	6.1	114	5.9	107	4.8
80	128	7.5	121	6.4	115	6.3	108	5.2

Table 4  
Heat capacities ( $\text{J mol}^{-1} \text{K}^{-1}$ ) of MEA (1) + 2-PE (2) +  $\text{H}_2\text{O}$  (3) for  $x_3 = 0.6$

$t$ ( $^{\circ}\text{C}$ )	$x_1/x_2 = 0.08/0.32$		$x_1/x_2 = 0.16/0.24$		$x_1/x_2 = 0.24/0.16$		$x_1/x_2 = 0.32/0.08$	
	$C_p$	$C_p^E$	$C_p$	$C_p^E$	$C_p$	$C_p^E$	$C_p$	$C_p^E$
30	157	4.7	146	3.8	135	2.9	123	1.0
35	159	5.3	147	3.5	136	2.8	125	2.0
40	161	6.2	149	4.6	138	4.0	126	2.4
45	163	6.8	151	5.4	139	3.9	128	3.5
50	165	7.4	153	6.2	141	5.0	129	3.8
55	167	8.3	154	6.2	143	6.0	130	3.9
60	168	7.9	156	7.0	144	6.1	132	5.3
65	170	8.4	158	7.7	146	7.0	133	5.3
70	172	9.4	160	8.8	147	7.2	135	6.7
75	174	10.0	161	8.7	149	8.3	136	7.0
80	176	10.5	163	9.3	151	9.2	138	8.0

various mole fractions of water from 0.2 to 0.8. The results are presented in Tables 3–6. The derived  $C_p^E$  from Eq. (1) for MEA (1) + 2-PE (2) +  $\text{H}_2\text{O}$  (3) are also presented in Tables 3–6. The values of  $C_p^E$  for MEA (1) + 2-PE (2) +  $\text{H}_2\text{O}$  (3) systems exhibit all positive values for all temperature range, as in Tables 3–6.

For a ternary system, the compositional dependence of the excess molar heat capacity is assumed as follows:

$$C_p^E = C_{p,12}^E + C_{p,13}^E + C_{p,23}^E + x_1x_2x_3(b_0 + b_1(T)) \quad (4)$$

For a binary system, any one of  $x_i$  equals zero, Eq. (4) reduces to Eq. (2). The parameters  $b_i$  determined from

$C_p^E$  of MEA (1) + 2-PE (2) +  $\text{H}_2\text{O}$  (3) are also presented in Table 2. Using Eq. (4) and parameters in Table 2, the result for  $C_p^E$  calculation (AAD%) for a total of 176 data points of MEA (1) + 2-PE (2) +  $\text{H}_2\text{O}$  (3) for  $C_p^E$  and  $C_p$  are 7.4 and 0.2%, respectively. Thus, the excess molar heat capacity for the MEA (1) + 2-PE (2) +  $\text{H}_2\text{O}$  (3) system can be satisfactorily represented by Eq. (4).

Plots of  $C_p^E$  for MEA (1) + 2-PE (2) +  $\text{H}_2\text{O}$  (3) for  $x_3$  equals to 0.6 and 0.4 for temperatures from 30 to 80  $^{\circ}\text{C}$  are shown in Figs. 3 and 4, respectively. The solid lines in Figs. 3 and 4 are calculated values from Eq. (4). As shown in Fig. 3 for  $x_3 = 0.6$ , the value of  $C_p^E$  for MEA (1) + 2-PE (2) +  $\text{H}_2\text{O}$  (3) increases as the temperature increases for a constant mole fraction of MEA; the value of  $C_p^E$  decreases as the mole

Table 5  
Heat capacities ( $\text{J mol}^{-1} \text{K}^{-1}$ ) of MEA (1) + 2-PE (2) +  $\text{H}_2\text{O}$  (3) for  $x_3 = 0.4$

$t$ ( $^{\circ}\text{C}$ )	$x_1/x_2 = 0.12/0.48$		$x_1/x_2 = 0.24/0.36$		$x_1/x_2 = 0.36/0.24$		$x_1/x_2 = 0.48/0.12$	
	$C_p$	$C_p^E$	$C_p$	$C_p^E$	$C_p$	$C_p^E$	$C_p$	$C_p^E$
30	196	5.2	180	4.3	165	4.5	148	2.6
35	198	5.1	182	4.4	167	4.8	149	2.1
40	200	5.5	185	6.1	168	4.7	151	3.3
45	203	6.3	187	6.2	170	5.0	153	3.9
50	205	6.3	189	6.5	172	5.7	154	3.9
55	208	7.6	191	6.9	174	6.2	156	4.6
60	210	7.5	193	7.2	176	6.9	158	5.6
65	213	8.4	196	8.3	178	7.2	159	5.1
70	215	8.8	198	8.9	180	8.1	161	6.3
75	217	8.7	200	9.2	182	8.8	163	7.3
80	220	9.5	202	9.3	184	9.1	164	6.8

Table 6  
Heat capacities ( $\text{J mol}^{-1} \text{K}^{-1}$ ) of MEA (1) + 2-PE (2) +  $\text{H}_2\text{O}$  (3) for  $x_3 = 0.2$

$t$ ( $^{\circ}\text{C}$ )	$x_1/x_2 = 0.16/0.64$		$x_1/x_2 = 0.32/0.48$		$x_1/x_2 = 0.48/0.32$		$x_1/x_2 = 0.64/0.16$	
	$C_p$	$C_p^E$	$C_p$	$C_p^E$	$C_p$	$C_p^E$	$C_p$	$C_p^E$
30	234	4.7	214	4.9	193	4.0	173	4.2
35	237	4.8	217	5.3	195	3.8	174	3.3
40	239	4.7	219	5.5	198	5.3	176	4.1
45	242	4.9	221	5.0	200	5.1	178	4.2
50	245	5.1	224	5.7	202	5.3	180	4.9
55	248	5.9	226	5.7	204	5.4	181	4.2
60	250	5.2	228	5.4	206	5.6	183	4.9
65	253	5.3	231	5.8	208	5.4	185	5.0
70	256	6.2	233	6.1	210	5.9	187	5.8
75	258	5.5	236	6.8	212	6.2	188	5.5
80	261	5.6	238	6.2	214	5.9	190	5.6

fraction of MEA increases at a constant temperature. As shown in Fig. 4 for  $x_3 = 0.4$ , the value of  $C_p^E$  increases as the mole fraction of MEA increases up to 0.12 for a constant temperature and decreases as the mole fraction of MEA increases for  $x_1 > 0.12$ .

As in a triangle plot in Fig. 5, the values of  $C_p^E$  for MEA (1) + 2-PE (2) +  $\text{H}_2\text{O}$  (3) calculated by Eq. (4)

for various values of  $C_p^E$  at  $80^{\circ}\text{C}$  are shown. It indicates that only the positive values of  $C_p^E$  occur at the entire concentration region at  $80^{\circ}\text{C}$ ; the largest value of  $C_p^E$  is found in the region of the low mole fraction of MEA, as shown in Fig. 5. In Fig. 6, the various temperatures at a constant value of  $C_p^E = 6.0 \text{ J mol}^{-1} \text{ K}^{-1}$  for MEA (1) + 2-PE (2) +  $\text{H}_2\text{O}$  (3) are shown. As shown in

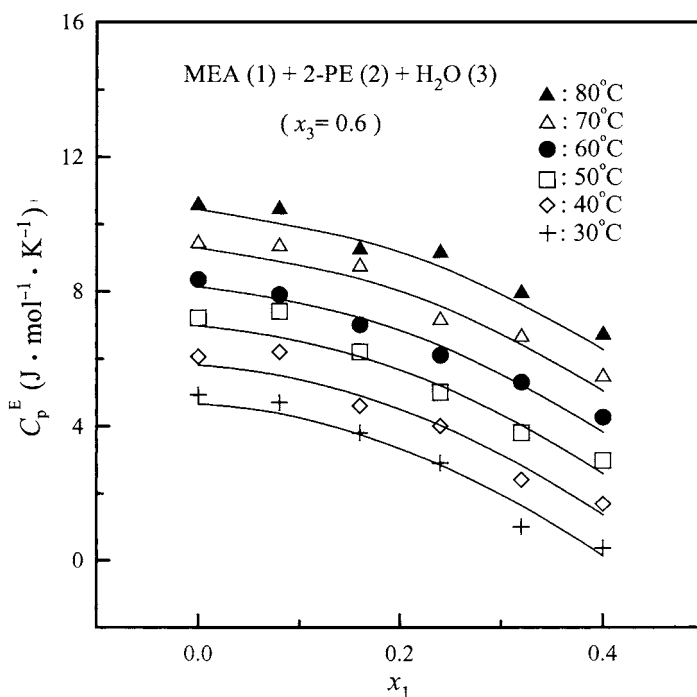


Fig. 3. Excess molar heat capacity of MEA (1) + 2-PE (2) +  $\text{H}_2\text{O}$  (3) as a function of mole fraction of MEA at  $x_3 = 0.6$ : symbols, derived values; lines, calculated using Eq. (4).

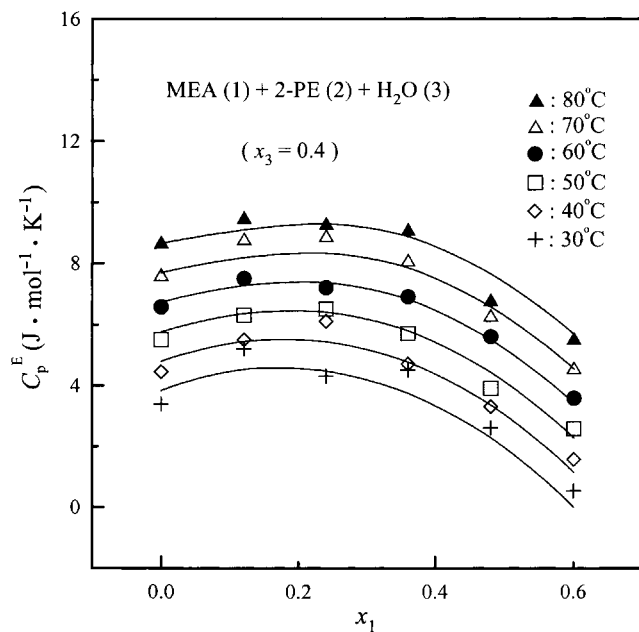


Fig. 4. Excess molar heat capacity of MEA (1) + 2-PE (2) + H<sub>2</sub>O (3) as a function of mole fraction of MEA at  $x_3 = 0.4$ : symbols, derived values; lines, calculated using Eq. (4).

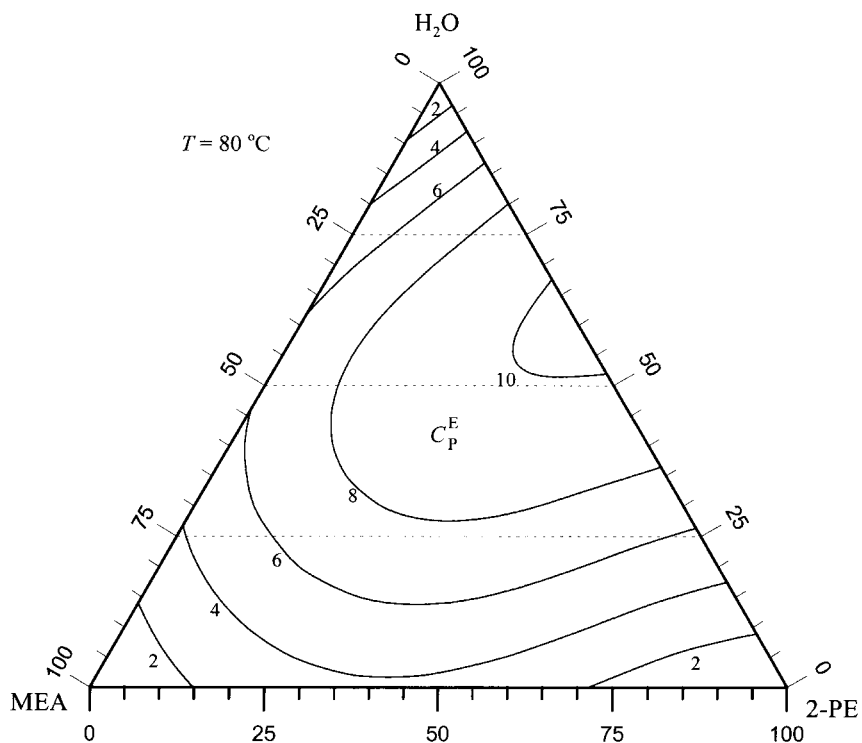


Fig. 5. Excess molar heat capacity of MEA (1) + 2-PE (2) + H<sub>2</sub>O (3) at constant 80 °C for various values of  $C_p^E$ ; lines are calculated using Eq. (4). The mole percentage of component is used for the axis label.

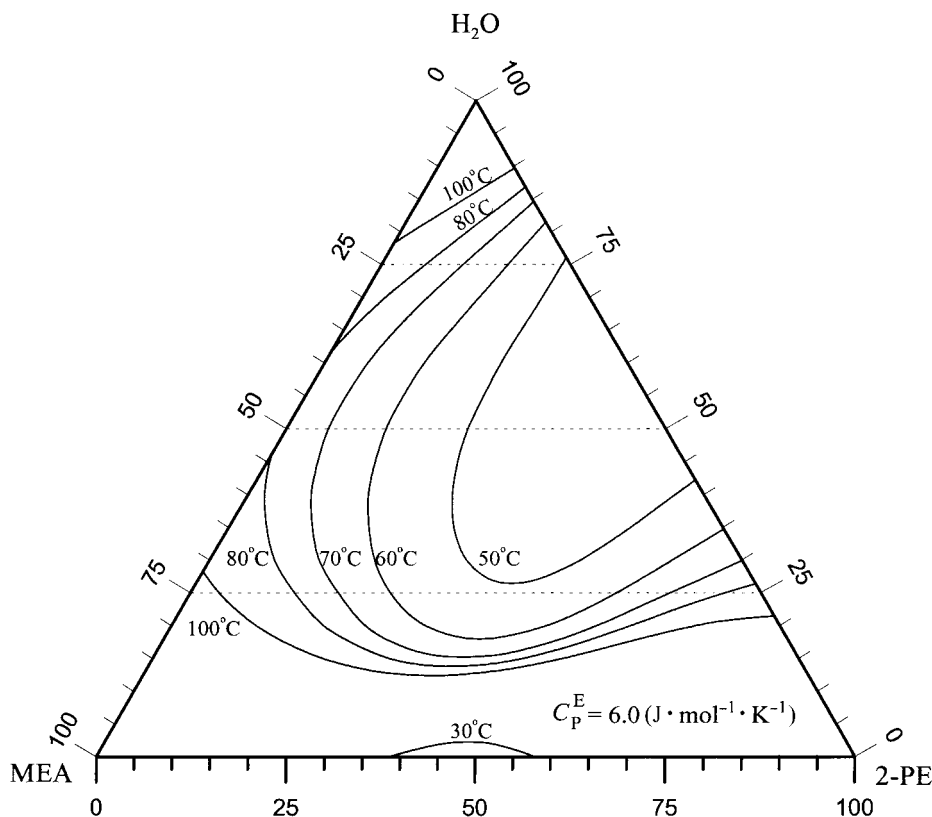


Fig. 6. Excess molar heat capacity of MEA (1) + 2-PE (2) + H<sub>2</sub>O (3) at constant  $C_p^E = 6.0 \text{ J mol}^{-1} \text{ K}^{-1}$  for temperatures from 30 to 100 °C: lines are calculated using Eq. (4). The mole percentage of component is used for the axis label.

Fig. 6, at the same  $C_p^E = 6.0 \text{ J mol}^{-1} \text{ K}^{-1}$  the isotherms distribute systematically along the path of the various concentrations.

#### 4. Conclusions

Heat capacities of aqueous mixtures of MEA with 2-PE were measured from 30 to 80 °C with a differential scanning calorimeter. An excess molar heat capacity expression using the Redlich–Kister equation for the composition dependence is used to represent the measured  $C_p$  of alkanolamine aqueous solutions. For a total of 176 data points, the results of calculation (overall average absolute percentage deviation) of the heat capacity for MEA + 2-PE + water system are 0.2 and 7.4% for molar heat capacity and excess molar heat capacity, respectively. The heat capacities of aqueous mixtures of MEA with 2-PE presented in this

study are, in general, of sufficient accuracy for most engineering-design calculations.

#### Acknowledgements

This research was supported by a grant, NSC 90-2214-E033-007, of the National Science Council of the Republic of China.

#### References

- [1] A.L. Kohl, F.C. Riesenfeld, Gas Purification, 4th Edition, Gulf, Houston, TX, 1985.
- [2] J.A. Riddick, W.B. Bunger, T.K. Sakano, Organic Solvents, 4th Edition, Wiley, New York, 1986.
- [3] L.L. Lee, Thermodynamic Models for Natural Gas Sweetening Fluids Annual report to the Gas Research Institute, Report No. GRI/94/0232, 1994.



- [4] D.R. Lide, Handbook of Organic Solvents, CRC Press, Boca Raton, 1995.
- [5] Y. Maham, L.G. Hepler, A.E. Mather, A.W. Hakin, R.A. Marriott, J. Chem. Soc. Faraday Trans. 93 (1997) 1747–1750.
- [6] L.F. Chiu, H.F. Liu, M.H. Li, J. Chem. Eng. Data 44 (1999) 631–636.
- [7] Union Carbide Chemical Co., Gas Treating Chemicals, Vol. 1, 1957.
- [8] R.H. Weiland, J.C. Dingman, D.B. Cronin, J. Chem. Eng. Data 42 (1997) 1004–1006.
- [9] L.F. Chiu, M.H. Li, J. Chem. Eng. Data 44 (1999) 1396–1401.
- [10] Texaco Chemical Co., Gas Treating Data Book, 1969.
- [11] T.A. Hayden, T.G.A. Smith, A.E. Mather, J. Chem. Eng. Data 28 (1983) 196–197.
- [12] Y.J. Chen, T.W. Shih, M.H. Li, J. Chem. Eng. Data 46 (2001) 51–55.
- [13] Y.J. Chen, M.H. Li, J. Chem. Eng. Data 46 (2001) 102–106.
- [14] T.W. Shih, M.H. Li, Fluid Phase Equilib., 2002, in press.
- [15] D.R. Lide, H.V. Kehiaian, CRC Handbook of Thermophysical and Thermochemical Data, CRC Press, Boca Raton, 1994.
- [16] N.S. Osborne, H.F. Stimson, D.C. Ginnings, J. Res. Nat. Bur. Stand. 23 (1939) 197–260.